B. B. Dumre, N. J. Szymanski, V. Adhikari, I. Khatri, D. Gall, S. V. Khare, Solar Energy 194, 742, Supplementary Material (2019)

Improved optoelectronic properties in $CdTe_{1-x}Se_x$ through controlled composition and short-range order

B. B. Dumre[a], N. J. Szymanski[a,b], V. Adhikari[a], I. Khatri[a], D. Gall[c], S. V. Khare[a,*]

[a]Department of Physics and Astronomy, University of Toledo, Toledo, OH 43606, USA

[b]Department of Material Science and Engineering, University of California, Berkeley, CA 94720-1760, USA

[c]Department of Materials Science and Engineering, Rensselaer Polytechnic Institute, Troy, NY 12180, USA

*Corresponding Author: sanjay.khare@utoledo.edu

Supplementary Material

(B. B. Dumre, N. J. Szymanski, V. Adhikari, I. Khatri, D. Gall, S. V. Khare, Solar Energy 194, 742, Supplementary Material (2019))

B. B. Dumre, N. J. Szymanski, V. Adhikari, I. Khatri, D. Gall, S. V. Khare, Solar Energy 194, 742, Supplementary Material (2019)

Table S1: Equilibrium lattice constants (in-plane *a* and out-of-plane *c*) of disordered $CdTe_{1-x}Se_x$ in the zincblende and wurtzite structures, computed within the framework of GGA. Experimental data, where available, is listed in parenthesis for comparison.

Material	Zincblende	Wurtzite		
x	*a* (Å)	*a* (Å)	*c* (Å)	*c/a*
0.00	6.624 (6.48[a], 6.54[b])	4.681 (4.57[c])	7.668 (7.47[c])	1.638
0.25	6.521	4.609	7.544	1.637
0.50	6.418	4.537	7.419	1.635
0.75	6.311	4.459	7.295	1.636
1.00	6.207 (6.052[d], 6.084[a])	4.391 (4.30[e])	7.166 (7.02[e])	1.632

a Ref. [108]

b Ref. [14]

c Ref. [109]

d Ref. [110]

e Ref. [111]

Table S2: Electronic band gaps of zincblende and wurtzite $CdSe_xTe_{1-x}$ computed using GGA and hybrid HSE06 functionals. Experimental data, where available, is listed in parentheses for comparison.

Material	Band Gap(eV)	
x	Wurtzite	Zinc Blende
0.00	0.56[a], 1.23[b] (1.59[c])	0.94[a], 1.54[b] (1.50[d])
0.25	0.84[a], 1.08[b]	0.86[a], 1.45[b]
0.50	0.76[a], 1.01[b]	0.81[a], 1.42[b]
0.75	0.77[a], 1.05[b]	0.85[a], 1.46[b]
1.00	1.06[a], 1.32[b] (1.70[e])	1.03[a], 1.61[b] (1.78[f])

[a] This work using GGA

[b] This work using HSEO6

[c] Ref. [94]

[d] Ref [20]

[e] Ref. [19]

[f] Ref. [93]

Table S3: Charge transfer (in elementary charge units *e*) from Cd to Te and Se in $CdSe_xTe_{1-x}$ calculated using the Bader charge partitioning scheme [77-80].

Structure	Zinc Blende		Wurtzite	
Composition (*x*)	Se	Te	Se	Te
0	N/A	0.52	N/A	0.51
0.25	0.72	0.52	0.72	0.51
0.50	0.72	0.51	0.72	0.52
0.75	0.72	0.51	0.72	0.51
1	0.70	N/A	0.71	N/A

Table S4: Average (DOS) effective masses of electrons and holes in zincblende and wurtzite $CdSe_xTe_{1-x}$. Units are in terms of the standard electron rest mass ($m_0 \approx 9.11\times10^{-31}$ kg), i.e., the effective electron mass is $m^* = m_e/m_0$ (and similar for holes, m_h).

Material	Zincblende		Wurtzite	
x	Electron	Hole	Electron	Hole
0.00	0.101	0.572	0.088	1.447
0.25	0.111	0.611	0.100	1.474
0.50	0.121	0.655	0.107	1.541
0.75	0.128	0.725	0.107	1.651
1.00	0.134	0.808	0.099	1.870

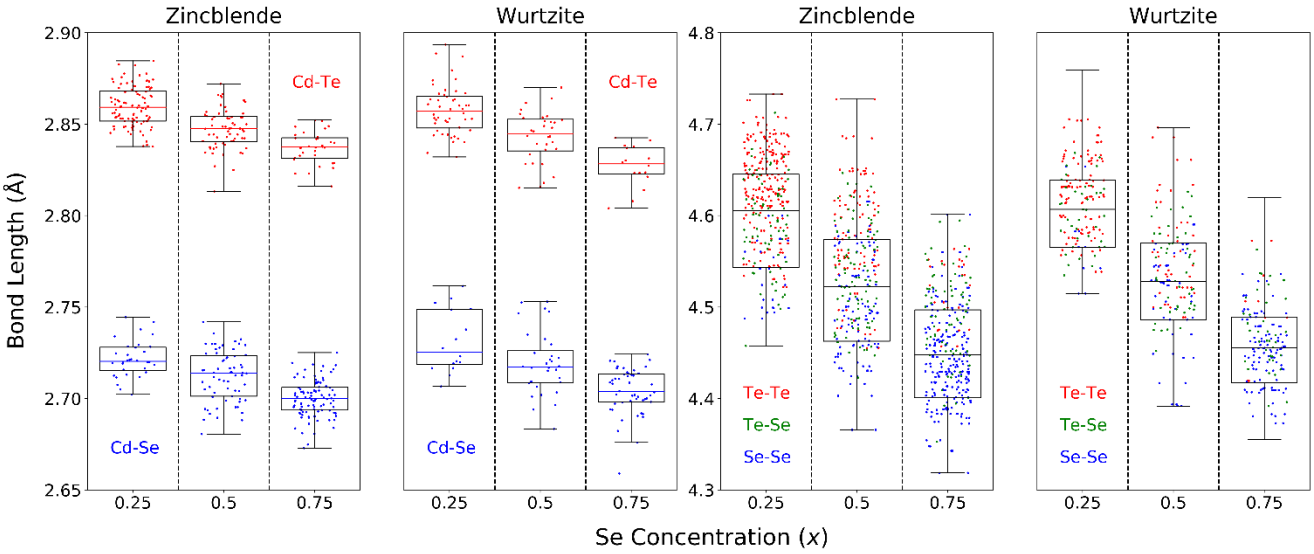

Figure S1: Box-and-whisker plots displaying the distribution of all unique bond lengths (Cd-Te, Cd-Se, Te-Te, Te-Se, Se-Se) within the disordered structures at intermediate concentrations (x = 0.25, 0.50, 0.75) simulated using special quasirandom structures.

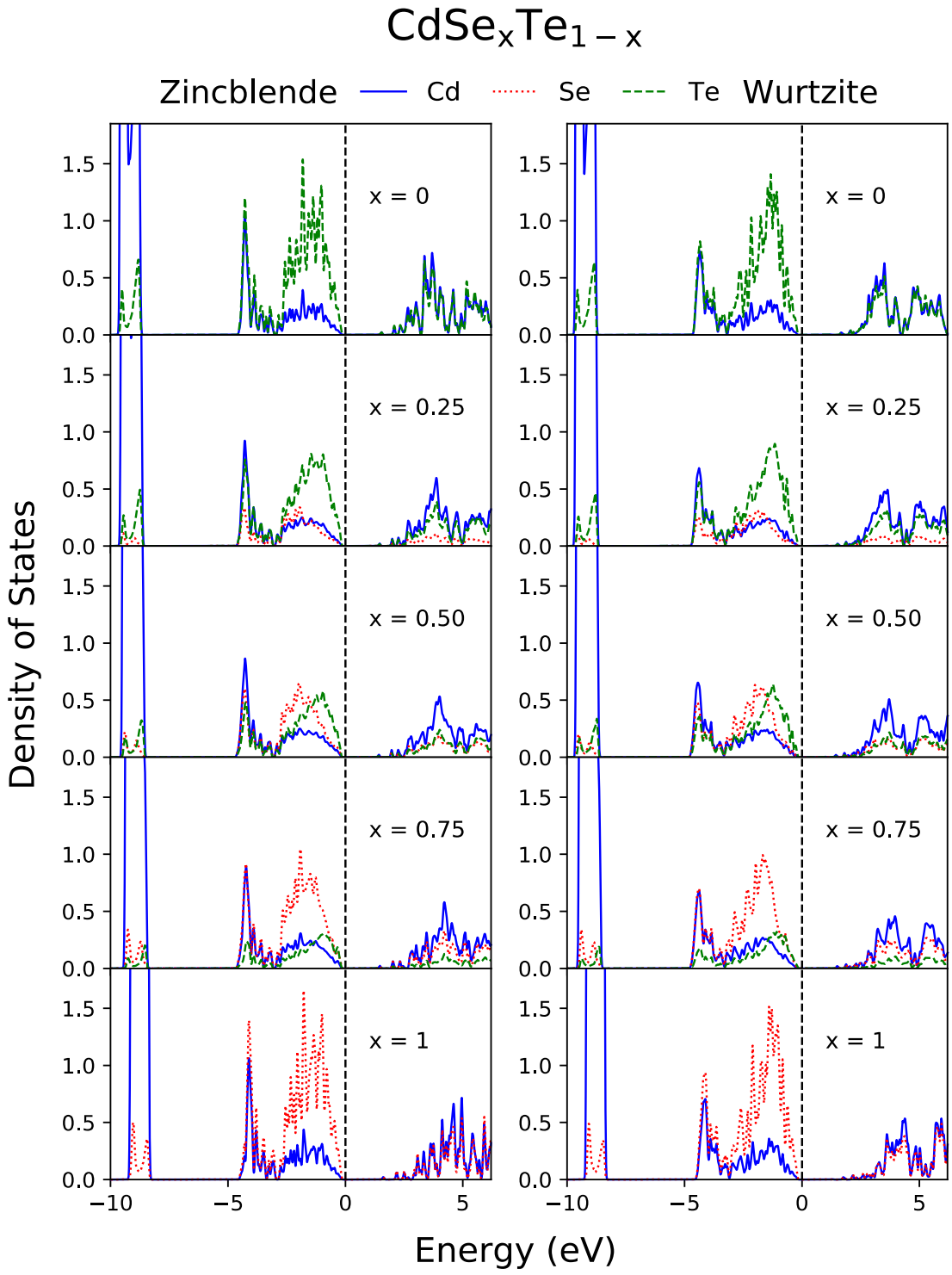

Figure S2: On-site electronic density of states per formula unit for each element for $CdSe_xTe_{1-x}$ in the zincblende and wurtzite structures, calculated using the hybrid HSE06 functional. The Fermi energy is set to 0 eV.

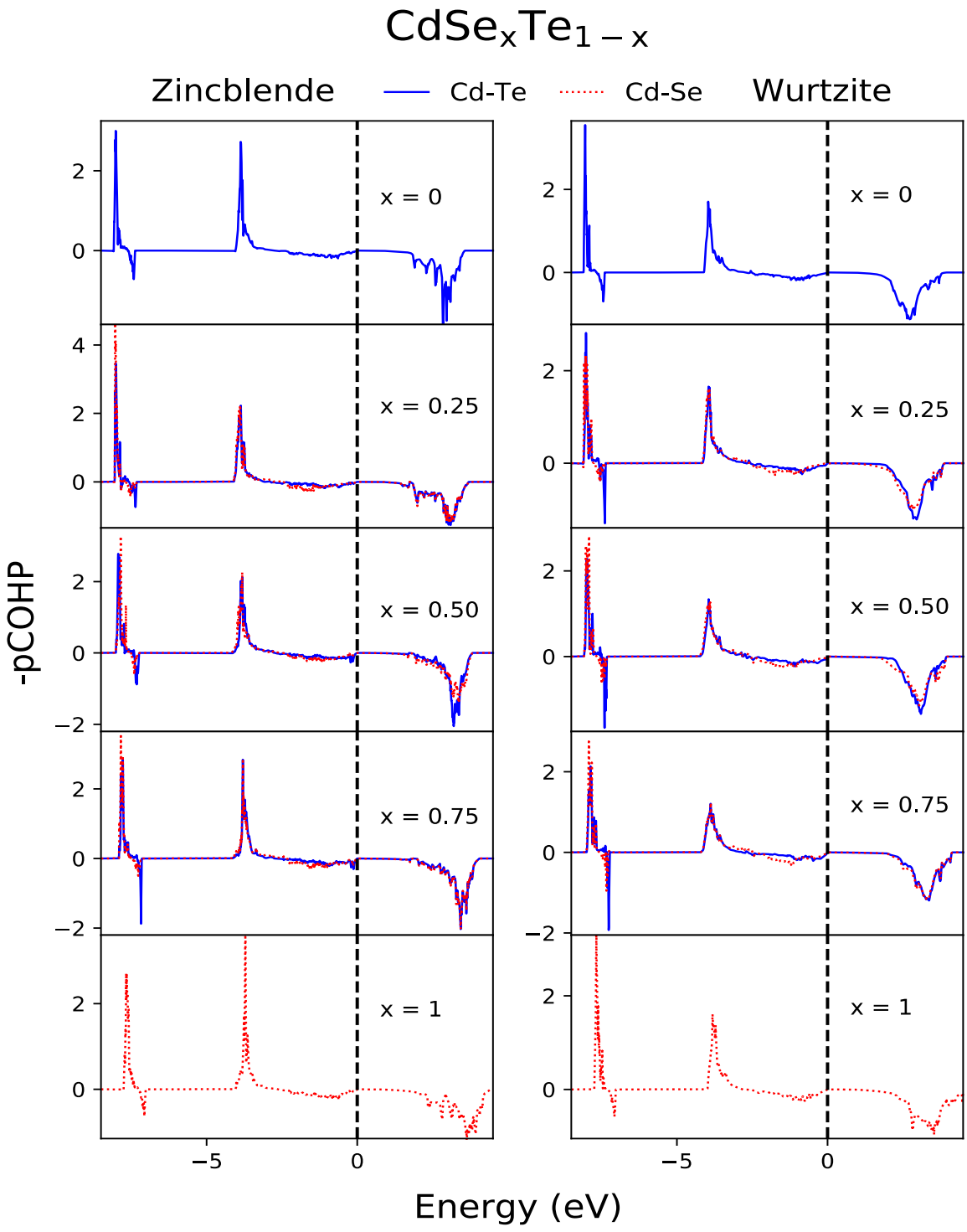

Figure S3: Projected Crystal Orbital Hamiltonian Populations (-pCOHP) of all nearest-neighbors in zincblende and wurtzite $CdSe_xTe_{1-x}$. Positive and negative values of -pCOHP correspond to bonding and antibonding interactions respectively. Cd-Te and Cd-Se pairs are shown, whereas all other covalent interactions are negligible. The Fermi energy is set to 0 eV.

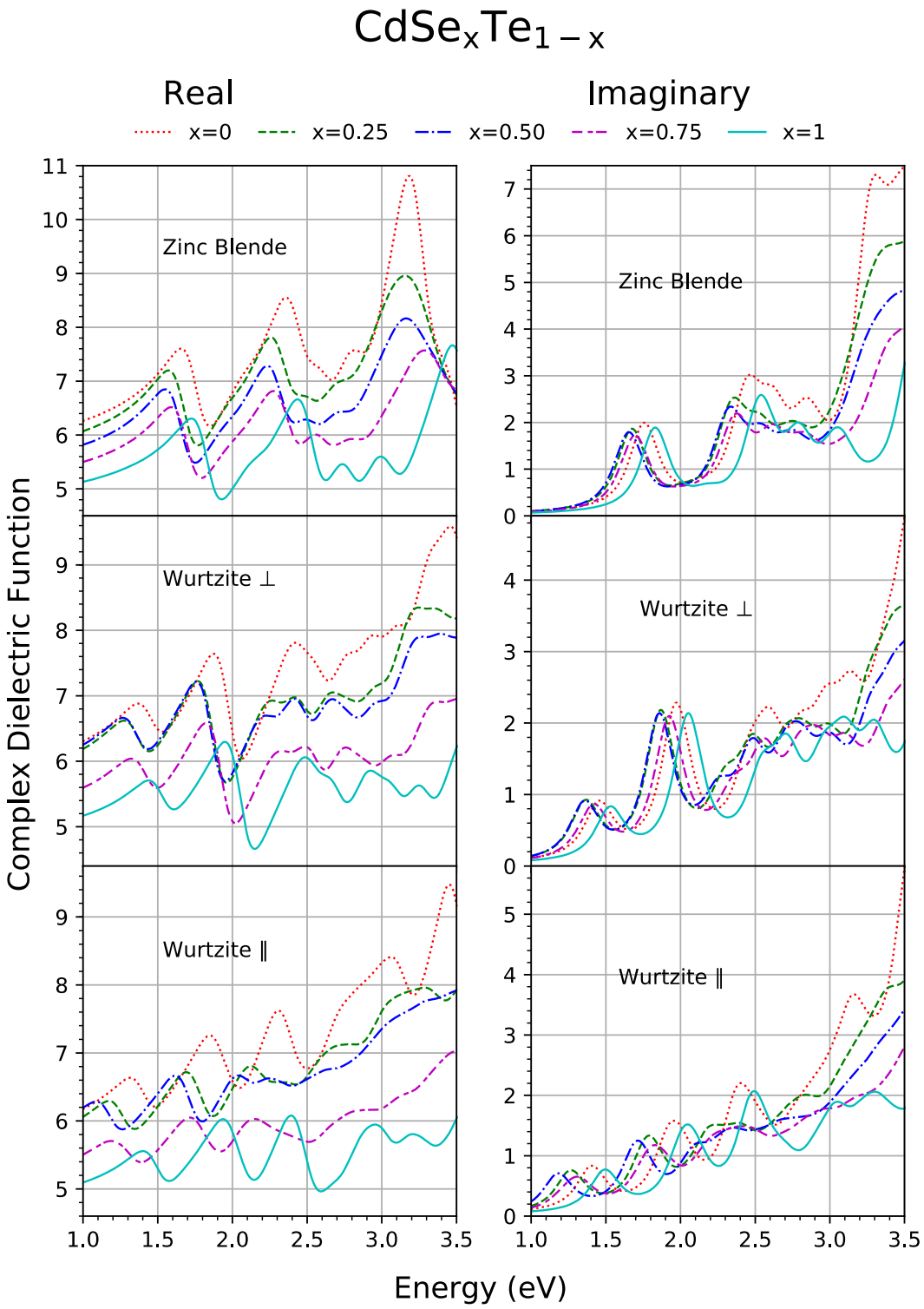

Fig S4: Complex dielectric functions for $CdSe_xTe_{1-x}$ in the zincblende and wurtzite structures, calculated using the hybrid HSE06 functional. Photon energies in the visible-UV range are shown.

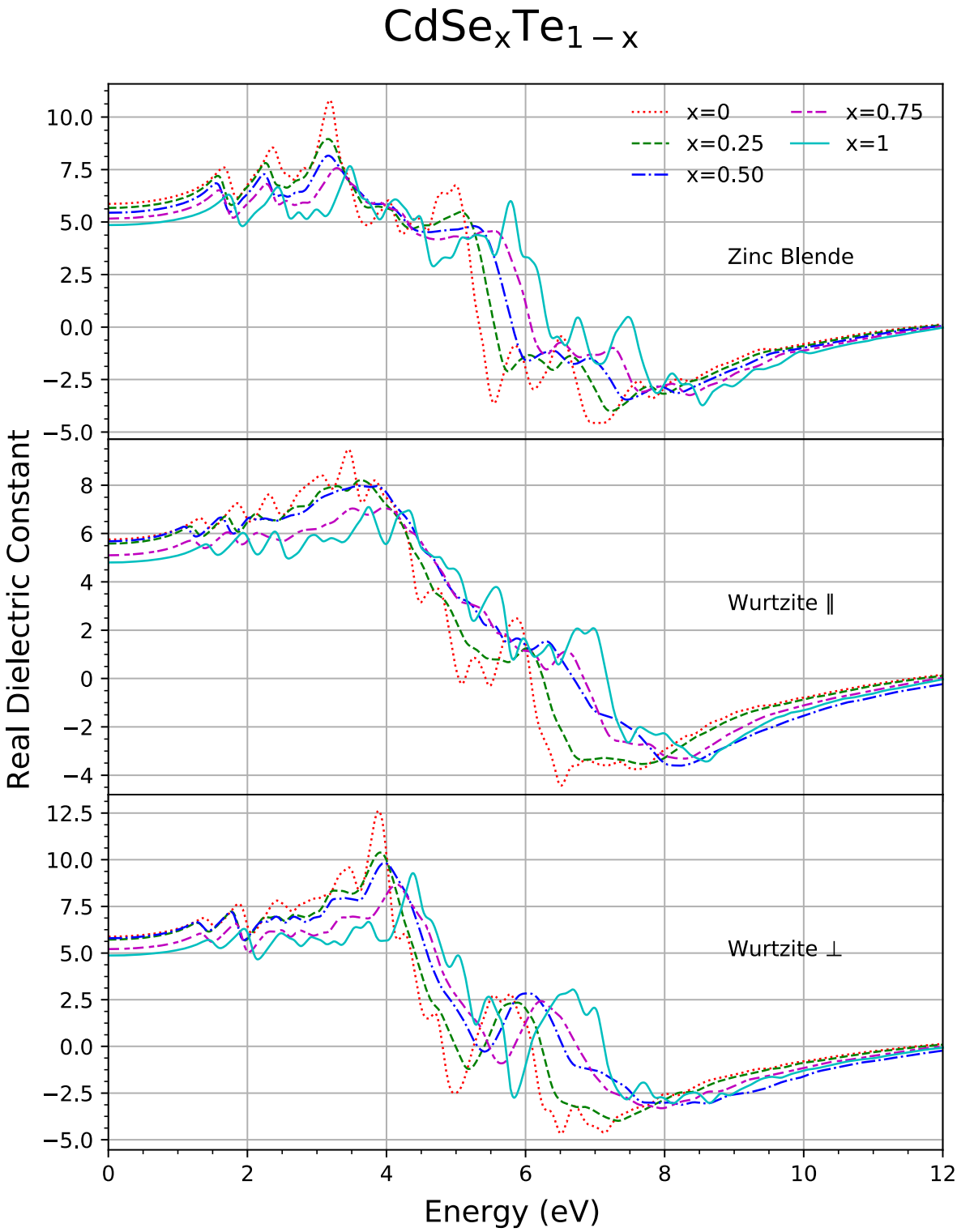

Fig S5: Variation of the real dielectric constants for $CdSe_xTe_{1-x}$ in the zincblende and wurtzite structures, calculated using the hybrid HSE06 functional.

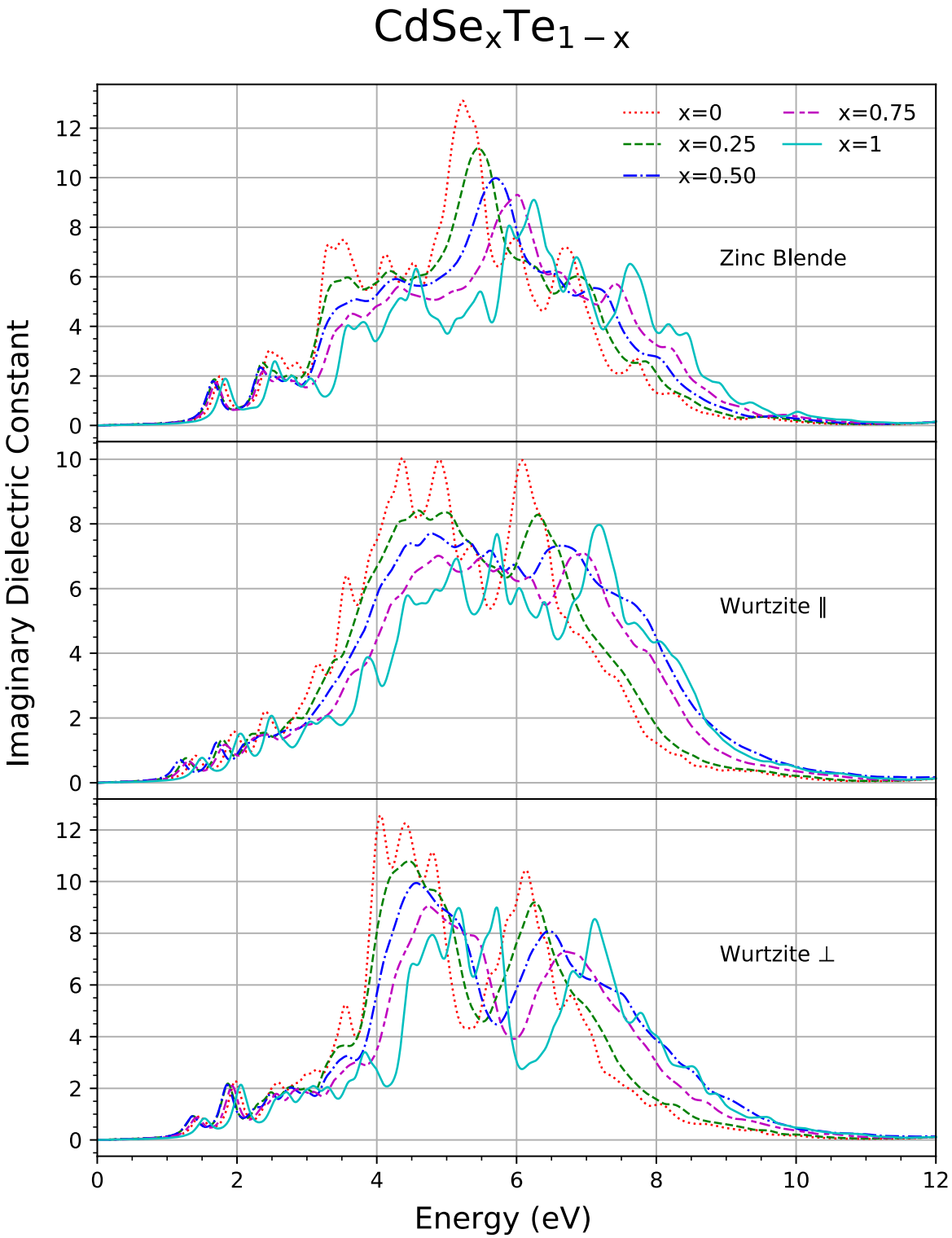

Fig S6: Variation of the imaginary dielectric constants for $CdSe_xTe_{1-x}$ in the zincblende and wurtzite structures, calculated using the hybrid HSE06 functional.